

Identifying Rodent Olfactory Bulb Structures with Micro-DTI

X.G. Zhao, E.S. Hui, K.C. Chan, K.X. Cai, H. Guo, P.T. Lai, E.X. Wu

Abstract—Olfactory bulb (OB) is one of the most developed systems in rodent models with complex neuronal organization and anatomical structures. MR diffusion tensor imaging (DTI) is a non-invasive technique to probe tissue microstructures by examining the diffusion characteristics of water molecules. This paper presents how different OB layers can be identified and quantitatively characterized by micro-DTI using a specially constructed micro-imaging radio frequency (RF) coil. High spatial resolution and high signal to noise ratio (SNR) DTI images of *ex vivo* rat OBs were obtained. Distinct contrasts were observed between various olfactory bulb layers in trace map, fractional anisotropy (FA) map and FA color map, all in consistence with the known OB neuroanatomy. These experimental results demonstrate the utility of micro-DTI in investigation of complex OB organization.

I. INTRODUCTION

Olfactory bulb (OB) is part of the olfactory system which receives, sorts and transduces odorant information from the external environment to deep brain structure in mammals [1]. The realization of such complicated functions depends on the axonal connection and projection: after the odorant molecules are received by olfactory receptor neurons (ORN) in the epithelium within the nasal cavity, the ORN axons, which form the most superficial layer, called olfactory nerve layer (ONL), transfer the odorant molecules to the glomerular layer (GL) [1, 2]. GL is responsible for the transduction and encoding of odor information. It is formed by spherical neuropil-rich bulbs surrounded by a shell of small neurons and glial cells. The glomeruli mainly comprise the dendrites of tufted cells, mitral cells, periglomerular cells and olfactory nerve terminals [1, 3]. Functioning as the output cells, tufted cells and mitral cells transmit the odor information to high order olfactory structure [1]. Granule cells form synapses on the soma and dendrites of mitral and tufted cells [4]. Granule cells are organized in columnar forms [5] and play the role in

X.G. Zhao, E.S. Hui, K.C. Chan, K.X. Cai and H. Guo are with the Laboratory of Biomedical Imaging and Signal Processing and the Department of Electrical and Electronic Engineering, The University of Hong Kong, Pokfulam, Hong Kong (e-mails: xggzhao@eee.hku.hk, h0202242@hkusua.hku.hk, kevin_ccw@hkusua.hku.hk, iinvivo@gmail.com and hua.guo@gmail.com).

P.T. Lai is with the Department of Electrical and Electronic Engineering, The University of Hong Kong, Pokfulam, Hong Kong (e-mails: laip@eee.hku.hk).

E.X. Wu is with the Laboratory of Biomedical Imaging and Signal Processing and the Department of Electrical and Electronic Engineering, The University of Hong Kong, Pokfulam, Hong Kong (corresponding author: (852) 2819-9713; fax: (852) 2819-9711; e-mail: ewu@eee.hku.hk)

Abbreviations: OB, olfactory bulb; ONL, olfactory nerve layer; ORN, olfactory receptor neuron; GL, glomerular layer; EPL, external plexiform layer; MCL, mitral cell layer; IPL, internal plexiform layer; GL, granular cell layer; EZ, ependymal zone.

olfactory neuron projection inhibition as periglomerular cells [6], as shown in Fig.1.

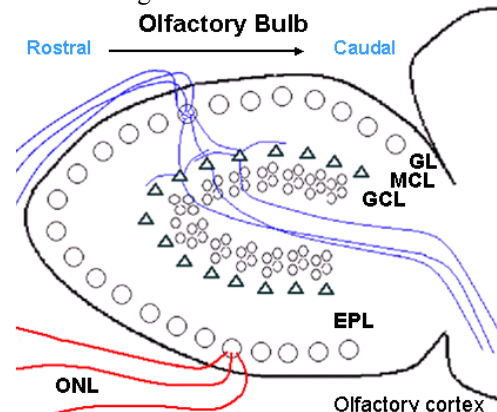


Fig.1. Neural pathway and organization inside olfactory bulb, shown in the sagittal orientation. GL: glomerular layer; MCL: mitral cell layer; GCL: granular cell layer; EPL: external plexiform layer; ONL: olfactory nerve layer.

Odor maps in GL has been studied with fMRI recently [7]. Manganese-enhanced MRI (MEMRI) was also performed to topographically trace structures inside OB [8]. However MR diffusion tensor imaging (DTI) has not been fully utilized to explore the organization of OB to our knowledge. DTI has been developed in recent years and employed extensively to study the anatomy [9] and pathological changes in the white matter of the central and peripheral nervous systems [10, 11]. Experimentally, it has been observed that trace, which is the sum of all eigenvalues of diffusion tensor, is inversely correlated to the cell density and axon density [12, 13].

In order to image OB with sufficient signal-to-noise ratios (SNR), a micro-imaging coil is required to limit noise from the background and thus increase SNR [14, 15]. Therefore, in this study we constructed a micro-imaging solenoid coil and acquired high spatial resolution and high SNR DTI data from *ex vivo* rat OB specimens. We quantitatively measured FA, trace, axial diffusivity and radial diffusivity values of the layers, and attempted to identify these layers with known anatomical structures of OB. We also performed acquisition comparison between the volume coil and our custom-made micro-imaging coil.

II. MATERIALS AND METHODOLOGY

A. OB sample preparations

Experiments were performed on female adult (295-320g) Sprague-Dawley rats (N=4). The rats were transcatheterially perfused with 0.9% saline, followed by PBS. After that, brains with intact olfactory bulbs were removed and

post-fixed in formalin for 24 hours. Brains were then placed into MR-compatible tubes and embedded in 1% agarose gel.

B. DTI data acquisition

All MR experiments were performed in a 7 Tesla MRI system (PharmaScan, Bruker, Germany). A custom-made two-loop circular coil of 10 mm diameter was used as a solenoid coil for both transmission and reception. Two trimmer capacitors were incorporated into the circuit to optimize tuning and matching. A transceiver volume coil of 23 mm inner diameter (Bruker, Germany) was used for SNR comparison with the custom-made micro-imaging coil.

A 2D diffusion-weighted (DW) spin echo sequence was used with the following acquisition parameters: FOV=25.6x25.6mm², image matrix=256x256 (zero-filled to 512x512), slice thickness/slice gap=0.4/0.1mm, TR/TE=3150/31 ms and NEX=10. DW images were acquired in 6 directions and 2 b-values were used (0 and 1500 s/mm²). The total scan time was 16 hours for each specimen. The image localization is shown in Fig. 2. When the volume coil was used for comparison, slice thickness was increased to 0.5 mm and the number of average was increased to 20 with a doubled scan time of 32 hours.

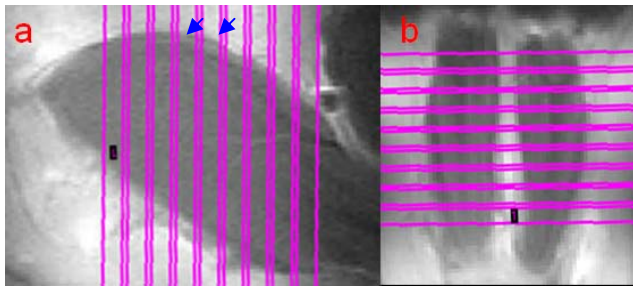


Fig.2. T₂-weighted images of an OB specimen in sagittal (a) and axial (b) views, and the corresponding slice locations for DTI scan.

C. Data analysis

DTI images were processed with DTI-studio v2.40 (<http://cmrm.med.jhmi.edu>, Johns Hopkins University, Baltimore, MD) to obtain trace, axial diffusivity, radial diffusivity, the color-coded FA and FA maps. Region-of-interest (ROIs) were manually drawn on 2 continuous slices in the centre of OB (as indicated by the blue arrows in Fig.2a) according to the contours of layers in color and trace maps using ImageJ software v1.38x. The measurements of the 2 slices of each layer were averaged. Data were compared using two-tailed paired student's t-tests, and the results were considered statistically significantly different when $P < 0.05$. Red, green and blue in the FA color maps represented the predominant diffusion direction of the structure from left to right, anterior to posterior, and rostral to caudal, respectively. SNR was calculated with the signal-background method [16] and compared through the T₂-weighted images of 6 slices with the two coils.

III. RESULT

Fig.3 shows trace, axial diffusivity, radial diffusivity, FA and

FA color maps of continuous coronal slices of an OB specimen with the slice locations indicated in Fig.2. All maps of the center slice (which is labeled with red rectangle in Fig.3) were enlarged for the convenience of showing more details and drawing ROI, as shown in Fig.4. Distinct contrast could be observed in trace, axial diffusivity, radial diffusivity and FA maps. With the order from the superficial to the deep OB structures as shown in FA color maps, the five distinct layers were labeled numerically (Fig.4).

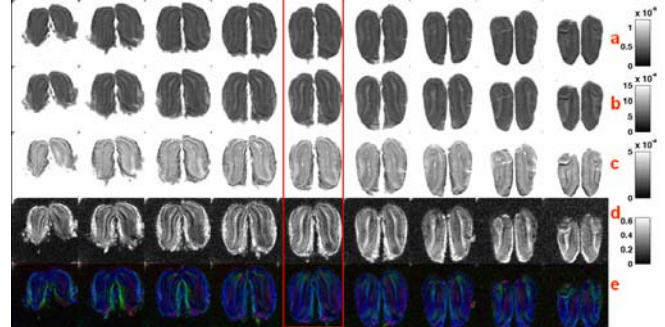


Fig.3. (a) Trace, (b) axial diffusivity, (c) radial diffusivity (d) FA, and (e) color maps of the OB specimen with slice locations shown in Fig.2. Images from left to right correspond to the slices from left to right indicated in Fig.2a and from down to up indicated in Fig.2b. In the FA color maps, red and green separately represent water diffusion in the left-right and anterior-posterior directions inside the plane; blue represents the rostral-caudal direction perpendicular with the plane.

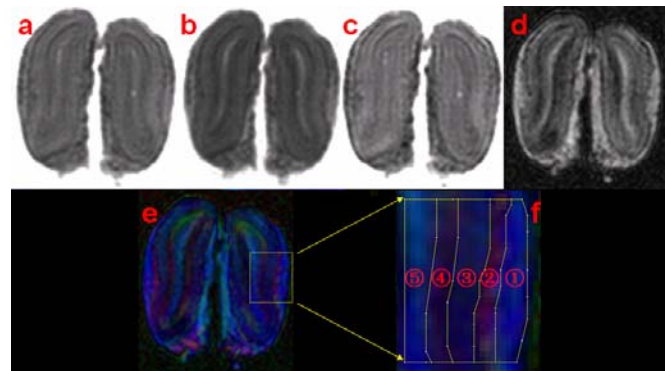


Fig.4. Enlarged (a) trace, (b) axial diffusivity, (c) radial diffusivity, (d) FA, and (e) FA color maps. The masks of different layers' contours were drawn out in the FA color map according to their colors, as shown in (f). The masks were used to label layers in other maps.

A. FA measurement and FA color map

Distinct orientations of anatomical structures were revealed in color-coded FA map. Quantitative assessment and identification of five OB layers were based on ROIs drawn in FA color maps. Averaged FA values of the five layers labeled in FA color map over four animals were measured, as shown in Fig.5. The result shows that the superficial layer (layer 1) and the deepest layer (layer 5), which showed blue colors in the color maps, had significantly higher FA values than the other layers ($P < 0.05$).

Though FA values of the other three layers were relatively comparable ($P > 0.05$) and were significantly lower than layers 1 and 5 ($P < 0.05$), their colors were apparently distinctive in the color map: layers 2 and 3 respectively were red and blue, while layer 4 was green on top and red in the middle in the

coronal view.

B. Trace, axial and radial diffusivity measurements

Five layers labeled in color map also showed distinct trace, axial diffusivity and radial diffusivity values. As shown in Fig.5, layers 2 and 4's trace and axial diffusivity values were lower than the other three ($P < 0.05$). Layers 1, 2 and 3's radial diffusivity values were lower than the other two ($P < 0.05$).

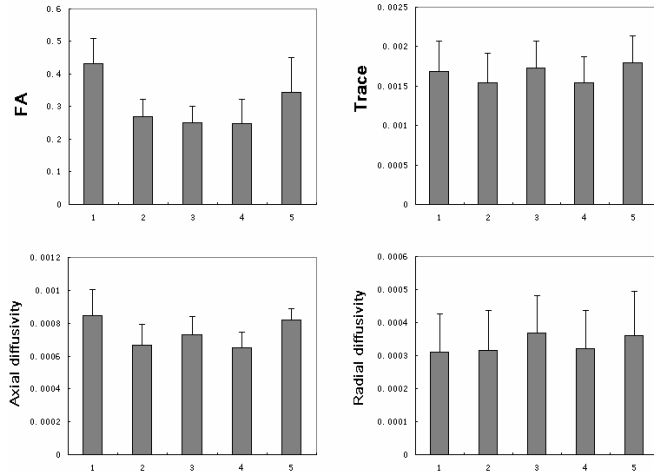


Fig.5. FA, trace, axial diffusivity and radial diffusivity of 5 layers shown in Fig.4. The values were averaged over all four animals with error bars indicating SDs. FA values in layer 1 and 5 were significantly ($P < 0.05$) higher than the others. No significant difference among FA values in layer 2, 3 and 4 ($P > 0.05$). Trace and axial diffusivity values in layer 2 and 4 were significantly ($P < 0.05$) lower than the other three. No significant difference among trace and axial diffusivity values in layer 1, 3 and 5 ($P > 0.05$). Radial diffusivity values in layer 1, 2 and 4 were significantly ($P < 0.05$) lower than the other two. No significant difference among radial diffusivity values in layer 1, 2 and 4 ($P > 0.05$).

Table 1. Morphology of the adult rat olfactory bulb in correlation with the DTI findings.

| Anatomic layer | Relative axon density [17] | Cell density (type) [1] | Main diffusion direction | Layer labeled in color map |
|----------------|----------------------------|-----------------------------|--------------------------|----------------------------|
| ONL | N/A | Low | rostral to caudal | 1 |
| GL | High | High (Periglomerular cells) | left to right | 2 |
| EPL | Low | Low | rostral to caudal | 3 |
| MCL | Moderate | Very high (Mitral cells) | N/A | N/A |
| IPL | moderate | Low | N/A | N/A |
| GCL | Low | Very high (granular cells) | Radial | 4 |
| EZ | Low | Low | rostral to caudal | 5 |

C. Layer identification

The layer identification result is shown in Table 1. Specifically, the superficial layer, layer 1, shows higher FA value than other layers in FA map (Fig. 5), which represents high anisotropy inside the structure [18]. It is blue in FA color map, which signifies the rostral to caudal diffusion direction. These characteristics tally with the anatomical superficial layer of OB, olfactory nerve layer (ONL), which

consists of olfactory receptor neuron (ORN) axons with rostral to caudal projection orientation to transmit odor information to the glomeruli [1].

Layer 5 is blue in color and has high FA value, which implies rostral to caudal diffusion direction and high anisotropy respectively, which matches its known structural characteristic. Topographically, olfactory ependymal zone (EZ) is the deepest layer in olfactory bulb which has trans-plane orientation and is also the pathway for output axons. The equivalent characteristics identify layer 5 with the olfactory ependymal zone.

Beneath ONL is layer 2, which corresponds to the anatomical layer, glomerular layer (GL). GL is immediately deep to ONL, in which ORN axons terminate onto dendrites of tufted and mitral cells. Its red color, representing left to right diffusion direction in FA color map, agrees with the transmission of odorant information from ONL to deeper layers. GL is a distinctive structure which has both high axon density [17] and cell density [1], as shown in Table 1. High axon and cell density will limit the diffusion of restricted water molecules, thus GL shows low value in trace map.

Layer 3, which is blue in FA color map, shows rostral to caudal diffusion direction. Axons of middle and deep tufted cells inside external plexiform layer (EPL) project out of the olfactory bulb to the anterior olfactory nucleus (AON) and other rostral olfactory cortical structures [1]. It is in agreement with the axonal direction illustrated by layer 3's blue color.

Immediately after the ependymal zone is layer 4. Radial columnar organization was reviewed in the color map: the top region shows green color representing anterior to posterior diffusion direction, and middle region shows red color representing left to right diffusion direction. This structure matches the organization of granular cell layer, which is organized in radial columnar forms [5].

D. Comparison between volume coil and custom-made micro-imaging coil

A comparison was performed between the volume coil and custom-made micro-imaging coil. SNR of the custom-made coil was 2.7 to 3.2 times as that of the volume coil using the signal-background method [16]. As shown in Fig.6, though the slice thickness with the volume coil is 0.1 mm thicker than that with the custom-made coil, and the scan time of volume coil was twice as that of the custom-made coil, the color map computed from DTI images acquired with the custom-made coil (Fig.6b) had much better quality than that of the volume coil.

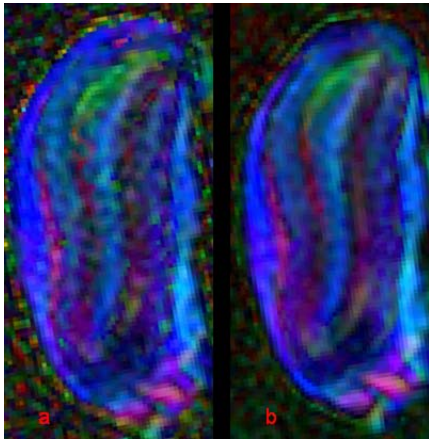


Fig.6. Comparison of FA color maps at the same slice location acquired with the volume coil (a), and the custom-made coil (b).

IV. DISCUSSION

Although the anatomical structures and neuronal functions of olfactory bulb have been documented in the past [1-5], the regional anisotropy and axonal orientations are not yet fully studied by any non-invasive techniques. Micro-DTI is sensitive to anisotropic diffusion of water and can be used to illustrate ordered structures. In this study we constructed a special micro-imaging coil, which not only enhances the image quality but also greatly reduces the scan time. Layers were identified by comparing the significant differences among distinct layers in trace maps, FA maps and FA color maps which are based on the axon and cell organization.

Five layers with different colors were observed in the FA color map, which in turn represented distinct diffusion directions, and possibly different anatomical structures. Our identification and quantitative assessment of olfactory bulb structures were based on the layers plotted in FA color map. We also attempted to examine the DTI data quantitatively by FA and trace values of each layer. As expected, the anisotropic characteristics revealed by FA and trace values in general agree with previously documented anatomical structure of olfactory bulb. The continuous slices in Fig.3 show the extension layers through the slice plane from the anterior part of olfactory bulb to deep brain structure. This corresponds with layer orientation known by anatomical techniques [1].

However, the identification was still limited by the resolution of the images. There are also another two anatomical layers: mitral cell layer (MCL) and internal plexiform layer (IPL) between EPL and GCL. The somata of mitral cells are 25-35 μm in diameter and are arranged in almost a monolayer with high density, and IPL is also a thin layer with low cell density [1]. It is difficult to unmistakably depict them with the current micro-DTI parameters.

SNR is an important parameter for MR imaging, especially for the MR diffusion tensor imaging. B_1 inhomogeneity is the main weakness of the two-loop solenoid coil. However, this problem is less detrimental while examining small objects but the SNR benefit is evident.

ACKNOWLEDGEMENT

The work was in part supported by Hong Kong Research Grant Council and HKU CRCG grants.

REFERENCES

- [1] M.T. Shipley and M. Ennis, "Functional organization of olfactory system," *J Neurobiol*, vol. 30, (no. 1), pp. 123-76, May 1996.
- [2] P. Mombaerts, F. Wang, C. Dulac, S.K. Chao, A. Nemes, M. Mendelsohn, J. Edmondson, and R. Axel, "Visualizing an olfactory sensory map," *Cell*, vol. 87, (no. 4), pp. 675-86, Nov 15 1996.
- [3] A.J. Pinching and T.P. Powell, "The neuropil of the glomeruli of the olfactory bulb," *J Cell Sci*, vol. 9, (no. 2), pp. 347-77, Sep 1971.
- [4] J.L. Price and T.P. Powell, "The synaptology of the granule cells of the olfactory bulb," *J Cell Sci*, vol. 7, (no. 1), pp. 125-55, Jul 1970.
- [5] D.C. Willhite, K.T. Nguyen, A.V. Masurkar, C.A. Greer, G.M. Shepherd, and W.R. Chen, "Viral tracing identifies distributed columnar organization in the olfactory bulb," *Proceedings of the National Academy of Sciences of the United States of America*, vol. 103, (no. 33), pp. 12592-7, Aug 15 2006.
- [6] J.L. Aungst, P.M. Heyward, A.C. Puche, S.V. Karnup, A. Hayar, G. Szabo, and M.T. Shipley, "Centre-surround inhibition among olfactory bulb glomeruli," *Nature*, vol. 426, (no. 6967), pp. 623-9, Dec 11 2003.
- [7] F. Xu, I. Kida, F. Hyder, and R.G. Shulman, "Assessment and discrimination of odor stimuli in rat olfactory bulb by dynamic functional MRI," *Proceedings of the National Academy of Sciences of the United States of America*, vol. 97, (no. 19), pp. 10601-6, Sep 12 2000.
- [8] R.G. Pautler and A.P. Koretsky, "Tracing odor-induced activation in the olfactory bulbs of mice using manganese-enhanced magnetic resonance imaging," *Neuroimage*, vol. 16, (no. 2), pp. 441-8, Jun 2002.
- [9] H. Huang, A. Yamamoto, M.A. Hossain, L. Younes, and S. Mori, "Quantitative cortical mapping of fractional anisotropy in developing rat brains," *J Neurosci*, vol. 28, (no. 6), pp. 1427-33, Feb 6 2008.
- [10] S.K. Song, S.W. Sun, M.J. Ramsbottom, C. Chang, J. Russell, and A.H. Cross, "Dysmyelination revealed through MRI as increased radial (but unchanged axial) diffusion of water," *Neuroimage*, vol. 17, (no. 3), pp. 1429-36, Nov 2002.
- [11] C. Beaulieu, M.D. Does, R.E. Snyder, and P.S. Allen, "Changes in water diffusion due to Wallerian degeneration in peripheral nerve," *Magn Reson Med*, vol. 36, (no. 4), pp. 627-31, Oct 1996.
- [12] R.K. Gupta, T.F. Cloughesy, U. Sinha, J. Garakian, J. Lazareff, G. Rubino, L. Rubino, D.P. Becker, H.V. Vinters, and J.R. Alger, "Relationships between choline magnetic resonance spectroscopy, apparent diffusion coefficient and quantitative histopathology in human glioma," *J Neurooncol*, vol. 50, (no. 3), pp. 215-26, Dec 2000.
- [13] C. Beaulieu and P.S. Allen, "Determinants of anisotropic water diffusion in nerves," *Magn Reson Med*, vol. 31, (no. 4), pp. 394-400, Apr 1994.
- [14] F.D. Doty, G. Entzminger, J. Kulkarni, K. Pamarthy, and J.P. Staab, "Radio frequency coil technology for small-animal MRI," *NMR Biomed*, vol. 20, (no. 3), pp. 304-25, May 2007.
- [15] C-NChen and D. Hoult, *Biomedical magnetic resonance technology*, New York: Institute of Physics Publishing, 1989.
- [16] D.W. McRobbie, E.A. Moore, M.J. Graves, and M.R. Prince, *MRI from picture to proton*, U. K.: Cambridge University Press, 2003.
- [17] J.H. McLean and M.T. Shipley, "Serotonergic afferents to the rat olfactory bulb: II. Changes in fiber distribution during development," *J Neurosci*, vol. 7, (no. 10), pp. 3029-39, Oct 1987.
- [18] P.J. Basser and C. Pierpaoli, "Microstructural and physiological features of tissues elucidated by quantitative-diffusion-tensor MRI," *J Magn Reson B*, vol. 111, (no. 3), pp. 209-19, Jun 1996.